

James Madison University

JMU Scholarly Commons

Department of Mathematics and Statistics -
Faculty Scholarship

Department of Mathematics and Statistics

2011

Shock-Associated Noise Generation in Curved Coanda Turbulent Wall Jets

Caroline P. Lubert

James Madison University, lubertcp@jmu.edu

Richard J. Shafer

Follow this and additional works at: <https://commons.lib.jmu.edu/mathstat>



Part of the [Aerospace Engineering Commons](#), and the [Applied Mathematics Commons](#)

Recommended Citation

Lubert, C., & Shafer, R. J. (2012). Shock Associated Noise Generation in Curved Turbulent Coanda Wall Jets. *Proceedings Of Meetings On Acoustics*, 14(1), 040002. DOI:10.1121/1.3675530

This Article is brought to you for free and open access by the Department of Mathematics and Statistics at JMU Scholarly Commons. It has been accepted for inclusion in Department of Mathematics and Statistics - Faculty Scholarship by an authorized administrator of JMU Scholarly Commons. For more information, please contact dc_admin@jmu.edu.

Shock Associated Noise Generation in Curved Turbulent Coanda Wall Jets

Caroline Lubert and Richard J. Shafer

Citation: [Proc. Mtgs. Acoust.](#) **14**, 040002 (2011); doi: 10.1121/1.3675530

View online: <http://dx.doi.org/10.1121/1.3675530>

View Table of Contents: <http://asa.scitation.org/toc/pma/14/1>

Published by the [Acoustical Society of America](#)

Proceedings of Meetings on Acoustics

Volume 14, 2011

<http://acousticalsociety.org/>

**162nd Meeting
Acoustical Society of America
San Diego, California
31 October - 4 November 2011
Session 5aNSa: Noise**

5aNSa5. Shock Associated Noise Generation in Curved Turbulent Coanda Wall Jets

Caroline Lubert* and Richard J. Shafer

***Corresponding author's address: Math & Stat, James Madison University, MSC 1911, Harrisonburg, VA 22807, lubertcp@jmu.edu**

Curved three-dimensional turbulent Coanda wall jets are present in a multitude of natural and engineering applications. The mechanism by which they form a shock-cell structure is poorly understood, as is the accompanying shock-associated noise (SAN) generation. This paper discusses these phenomena from both a modeling and experimental perspective. The Method of Characteristics is used to rewrite the governing hyperbolic partial differential equations as ordinary differential equations, which are then solved numerically using the Euler predictor-corrector method. The effects of complicating factors -- such as radial expansion and streamline curvature -- on the prediction of shock-cell location are then discussed. This paper next compares the theoretical calculations of the shock-wave structure with associated schlieren flow visualization results. Related acoustical measurements are also addressed. In this way, critical flow characteristics for shock-cell formation are identified, and their influence on SAN discussed.

Published by the Acoustical Society of America through the American Institute of Physics

1. INTRODUCTION

1.1 Coanda Flows

The Coanda effect was discovered early in the twentieth century by Romanian mathematician and scientist Henri Coanda, who described it as the phenomenon whereby "...when a jet is passed over a curved surface it bends to follow the surface, entraining large amounts of air as it does so..." [1]. The substantial flow deflection offered by the Coanda principle is generally accompanied by enhanced levels of turbulence and increased entrainment. A related, although generally undesirable, side-effect is the significant increase in associated noise levels. It is suggested [2] that this has prevented the Coanda effect from being more widely applied. The present work is part of an effort to better understand the mechanisms behind the aerodynamic noise generation in such jets, with the goal of facilitating improvements in the prediction and attenuation of such noise.

The jet under consideration here is assumed to issue at high velocity from an annular exit slot. Immediately upon exit it is adjacent to a solid three-dimensional Coanda surface. The geometry of interest is shown in Figure 1.

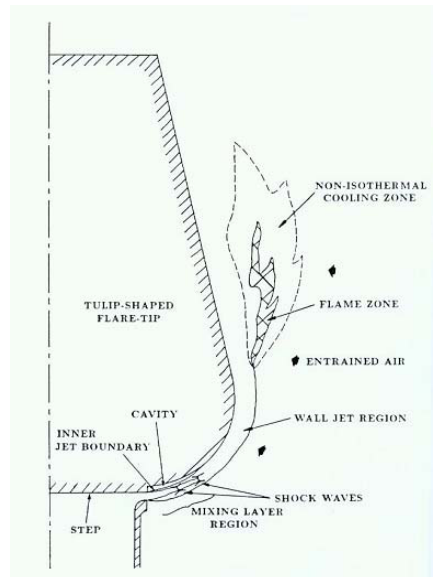


Figure 1: The flow field and combustion zone of a Coanda Flare

Although this representation is that of a Coanda flare [3,4] of the type used in the petroleum industry (an example of which is shown in operation in Figure 2), the experimental results and models developed herein can easily be applied to other examples of three-dimensional jet flows over turbulent Coanda surfaces.



Figure 2: An operating Coanda Flare

Jet flows such as that shown in Figure 1 emit both low- and high-frequency noise. It is the latter that is of greatest interest, since it is both the most annoying to the human ear, and the easiest to attenuate. There are two primary high-frequency noise sources; turbulent mixing noise (TMN) and shock-associated noise (SAN). The former has previously been discussed at length [5,6,7]. This paper presents the results of a preliminary investigation into the SAN generated by the mixing layer of a three-dimensional turbulent jet flowing adjacent to a solid Coanda surface.

1.2 Shock-Associated Noise (SAN)

In contrast to subsonic jets, conditions at a downstream point in a supersonic jet cannot affect those upstream. In this way, discontinuities in flow properties can arise. Depending upon the relative pressure difference between the nozzle exit pressure (p_e) and the ambient pressure (p_a) a stationary shock-cell structure is formed in the mixing layer region close to the jet exit slot. The interaction of downstream propagating turbulent eddies with this structure generates the high-frequency sound known as shock-associated noise. When the flow is three-dimensional, complicating factors such as radial expansion and streamline curvature are present. For a preliminary investigation into the nature and behavior of SAN we will assume that the jet is two-dimensional, as shown in Figure 1.

2. SHOCK WAVES IN COANDA FLOWS

2.1 Shock-Wave Generation

Consider an under-expanded jet. In this case, $p_e > p_a$ and a fan of expansion waves (waves such that the pressure and density of a base flow decrease on crossing them) will be generated at the lip of the nozzle exit slot. On interacting with a free jet boundary, the expansion waves cause the boundary to be displaced outwards, and this effect can be seen in the Schlieren flow visualization photograph of Figure 3.

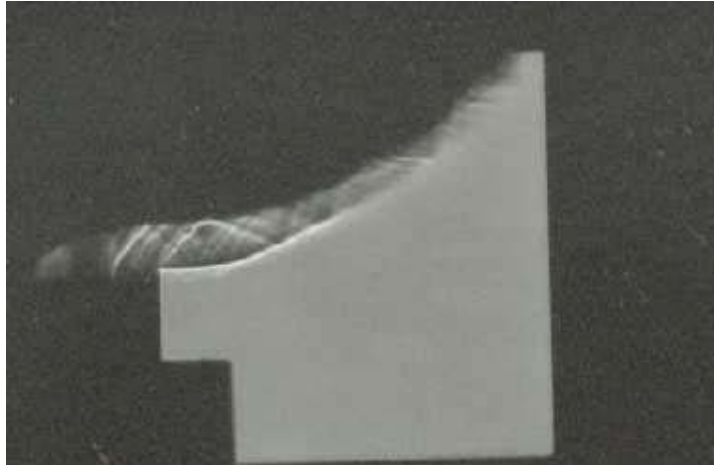


Figure 3: Typical flow structure in Coanda flare mixing layer

The expansion waves will reflect as either expansion or compression waves as they interact with a boundary. In order to preserve constant pressure at the jet boundary, the incident and reflected waves will be of opposite kinds and so an expansion wave reflects as a compression wave (pressure and density increase on crossing it) and vice versa. However, when a wave reflects from a solid surface, zero normal velocity must be preserved at the wall, and so an expansion wavefront will be reflected as an expansion wavefront, for example. The coalescence of these compression waves forms shock-waves, which reflect as shock waves from a solid surface and as expansion waves from a free jet boundary. This pattern of expansion, compression and shock-waves repeats itself periodically.

2.2 Coanda Flare Shock-Cell Formation

The flow under consideration in the current work is that associated with a turbulent Coanda flare of the type shown in Figure 1. Green [8] has shown that one-dimensional flow theory can be used to describe the flow through a convergent-divergent nozzle of the kind present in the Coanda flare. Thus, the jet emerging from the exit slot is supersonic for almost all operating pressures, and shock-waves are formed in the vicinity of the nozzle exit as described previously. The exact location of these shock-waves depends upon a variety of factors including the relative magnitudes of the pressure in the reservoir supplying the nozzle (p_0) and the pressure of the medium into which the jet flows, known as the ambient or back pressure (p_a).

In the case of the flare jet, a pattern of expansion, compression and shock-waves is present under a wide range of operating conditions. The quasi-periodic constituents of this pattern, known as shock cells, are shown schematically for a Coanda flare jet in Figure 4. Typically a series of 8-10 shock cells will form in the jet exhaust. Turbulent eddies convected downstream within the mixing layer region of the jet cause these shocks to be deformed. This distortion of the shock front propagates away as broadband, but strongly peaked sound waves known as Shock-Associated Noise (SAN). Shock-associated noise has several interesting aspects. Firstly there is a strong directivity associated with the SAN emitted by moving sound waves. It has been observed [9] that a turbulent eddy can successively interact with several shock waves, generating multiple sound sources (one resulting from each interaction). Additionally, a feedback cycle is often

present, leading to the generation of discrete, harmonically related tones known as screech tones.

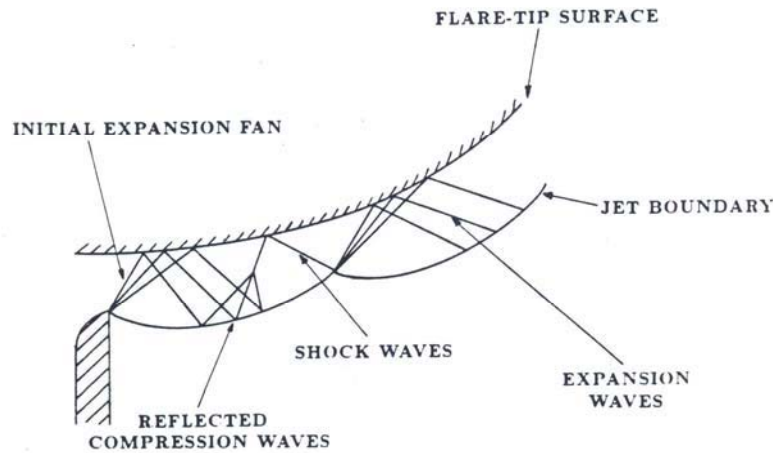


Figure 4: Shock cell structure near the exit slot of the flare (reproduced from [5])

The modelling of the shock-cell structure within a Coanda flare jet will now be discussed in more detail.

2.3 Shock-Cell Prediction

Theory: Method of Characteristics

For a steady two-dimensional irrotational flow, such as the one under consideration here, the governing equations are the speed of sound relationship,

$$a = a(\mathbf{V}) = a(u, v) \quad (1)$$

an equation expressing irrotationality:

$$u_y - v_x = 0 \quad (2)$$

and the Gas Dynamic equation:

$$(u^2 - a^2)u_x + (v^2 - a^2)v_y + 2uvu_y - \frac{\delta a^2 v}{y} = 0 \quad (3)$$

where $\delta = 0$ in planar flow and $\delta = 1$ for axisymmetric flow. (x, y) is the location of a point of interest and (u, v) are the velocity components of \mathbf{V} at this location.

This is a system of two coupled quasi-linear nonhomogeneous partial differential equations (PDEs) of the first-order in two independent variables, x and y . Note that in this context, 'quasi-linear ... of the first-order' means that a PDE is non-linear in the dependent variables (u and v , the flow velocity components) but linear in the first partial derivatives, (u_x, u_y, v_x, v_y) of these dependent variables.

The latter two equations ((2) and (3)) govern both subsonic and supersonic flow. However, the coefficients of the various derivatives are such that the mathematical type of the PDEs changes from elliptic when $M < 1$ (i.e. subsonic flow) to hyperbolic for supersonic flow ($M > 1$). For the two-dimensional supersonic turbulent Coanda flow under consideration, these hyperbolic PDEs can be solved using the Method of Characteristics. Such equations have the property that they can be reduced to ordinary differential equations (ODEs) known as compatibility equations, which are valid along specific, related, curves known as characteristics. Physically,

characteristics represent the path of propagation of a physical disturbance.

For a steady two-dimensional irrotational flow, the governing equations (1) – (3) yield compatibility equations

$$(u_{\pm}^2 - a_{\pm}^2)du_{\pm} + [2u_{\pm}v_{\pm} - (u_{\pm}^2 - a_{\pm}^2)\lambda_{\pm}]dv_{\pm} - \left(\frac{a_{\pm}^2 v_{\pm}}{y_{\pm}}\right)dx_{\pm} = 0 \quad (4)$$

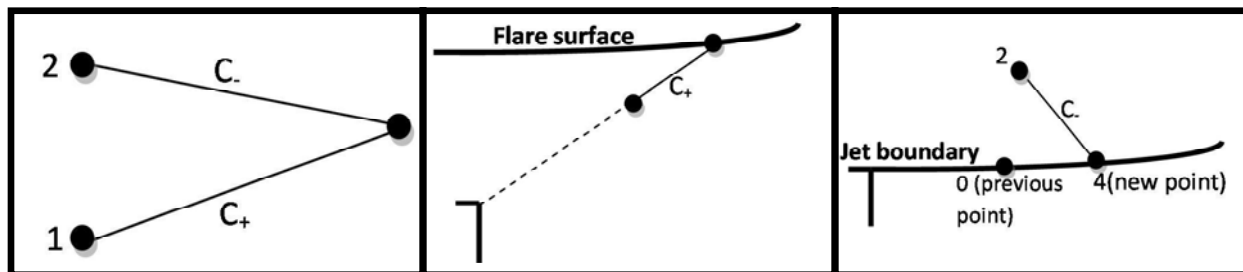
which are valid along the C_+ (where + denotes direction towards flare tip surface) and C_- (away from surface) characteristics described by:

$$\frac{dy}{dx_{\pm}} = \tan(\theta_{\pm} \mp \alpha_{\pm}) \quad (5)$$

θ_{\pm} is the angle that the flow streamline makes with the x-axis and α_{\pm} is the Mach angle. In the case of a supersonic flow, the characteristics are the Mach lines of the flow. Since equations (4) and (5) are non-linear, they must be discretized and solved by numerical means. In the present work, following Green [8] the Euler predictor-corrector method is used. This will now be discussed in more detail.

Numerical solution: Euler predictor-corrector method

At each point (x, y) along the characteristics given by (5), the velocity components (u, v) associated with that location (x, y) must be determined. In order to do so, the region of interest must be divided into three separate areas; interior points (which have both C_+ and C_- characteristics), wall points (which have only C_+ characteristics) and jet boundary points (with only C_- characteristics).



(a) Interior point

(b) wall point

(c) jet boundary point

Figure 5: Finite Difference schemes

Numerical determination of the location of the shock cells in a Coanda flare jet is then based on a modified Euler predictor-corrector finite difference iterative algorithm. The method is initialized with the number of lines in the initial expansion fan and the number of characteristics in the exit plane. The prediction step calculates a rough approximation of the desired quantities (x,y) and (u,v) by using their known initial values (at points 1 and 2 in Figure 5(a), for example) together with characteristic and compatibility equations to find values at a new point (via interim values). The corrector step then averages these predictor values with the initial values to get better estimates of interim values, and uses these to re-estimate values of (x,y) and (u,v) at the new point. The corrector step iterates until the desired stopping criteria are reached. Repeating

this process in a systematic way along each expansion fan, shock waves are formed where the velocity vectors coalesce.

2.4 Experimental Results

Experiments were conducted in a 5m x 2.5m x 2.5m anechoic chamber. The Coanda surface had a 53.3 mm maximum diameter. The operating pressures were between 5 and 40 psig, and the exit slot varied from 1.14mm to 4.19mm. All experiments were carried out at ambient (room) temperature and pressure. Simultaneous sound measurements and Schlieren flow visualization experiments were conducted as shown in Figure 6. Shock-cells formation was observed under almost all operating conditions.

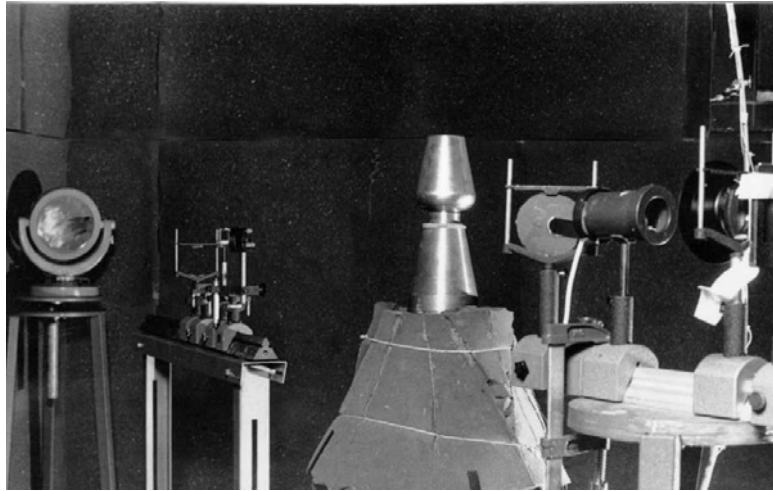


Figure 6: Anechoic chamber at JMU

A typical Schlieren image is shown in Figure 7 and the associated noise spectrum is shown in Figure 8.

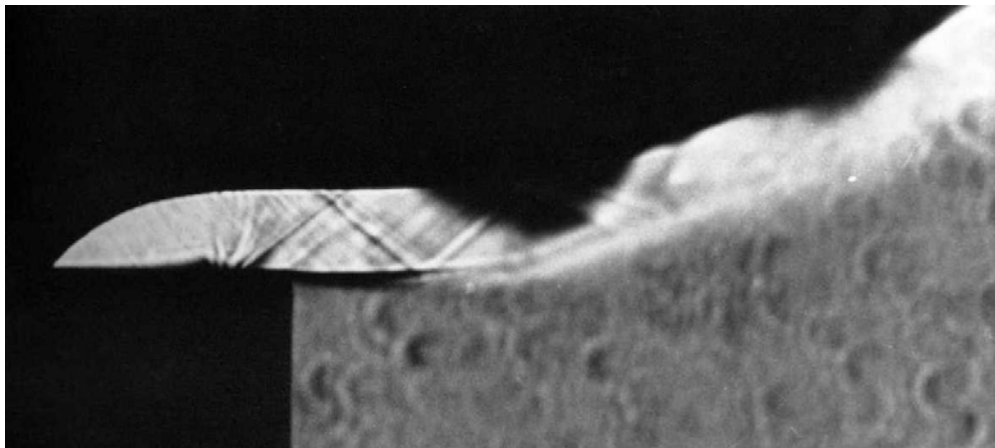


Figure 7: Typical Schlieren flow visualisation image

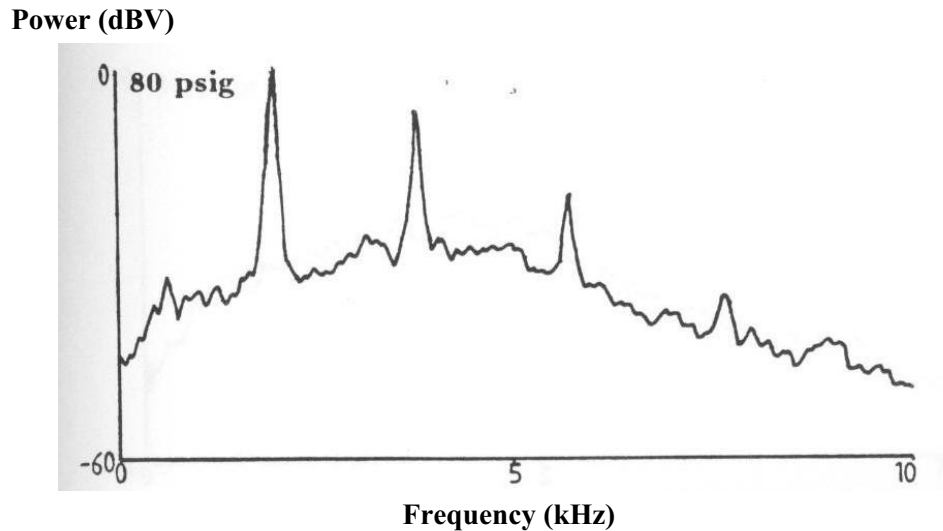
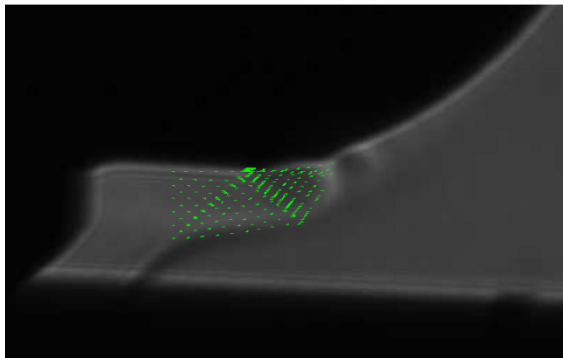
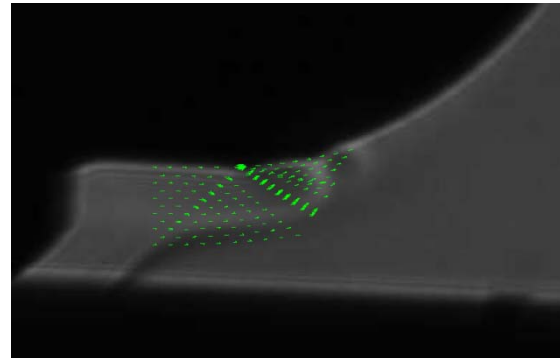


Figure 8: Flare spectrum (4 inch diameter, 15mm slot width, operating pressure 80 psig)

Shock cells are clearly seen in Figure 7, and the interaction of large-scale coherent structures with these shock cells produces both broadband and discrete SAN, as shown in Figure 8. Figure 9 shows the shock-cell location (predicted as described in Section 2.3) superimposed on experimental results similar to those of Figure 7. The arrows represent the (u,v) vectors at each point predicted by the intersections of characteristics, starting with the flow in the exit plane as well as the initial expansion fan. Shock waves are formed at the coalescence of these vectors and both the dark regions on the flow visualization figures, and the higher concentration of vectors (shown in blue) correspond to regions of higher pressure.



(a) 2.82mm slot width



(b) 3.23mm slot width

Figure 9: Comparison of experimental and theoretical results

Comparison indicates that this preliminary model is relatively accurate at predicting the location of the first shock cell formation. Cells further from the exit slot are less well predicted, and future work will focus on modifying this preliminary model to include radial expansion and streamline curvature, which is anticipated to improve these predictions.

3. SUMMARY AND CONCLUSIONS

This paper has presented the results of a preliminary investigation into the shock-associated noise generation in Coanda wall jets. To date, the model predicts the shock-cell formation reasonably well, at least for the cell nearest the exit slot. Work is currently underway to improve the model through inclusion of the complicating factors observed in a real Coanda flare jet, and relaxation of the assumption of two-dimensionality. These improved shock cell calculations will then be integrated into more complex model for predicting the SAN associated with turbulent Coanda flows.

REFERENCES

1. Coanda, H., Procédé de propulsion dans un fluide, Brevet Invent. Gr. Cl. 2, no. 762688 République Française, (1932).
2. Lubert, C.P, Application of Turbulent Mixing Noise Theory to Flows over Coanda Surfaces, Int. J. Acoustics and Vibration, 13(1), pp17-30, (2008).
3. Desty, D.H. No smoke without fire, Proceedings of the Institution of Mechanical Engineers, 197A, 159-170, (1983).
4. Desty, D.H, Boden, J.C. and Witheridge, R.E. The origination, development and application of novel premixed flare burners employing the Coanda effect, 85th Nat. AIChE meeting, Philadelphia, (1978).
5. Parsons, C. An experimental and theoretical study of the aeroacoustics of external-Coanda gas flares, Ph.D. Thesis, University of Exeter, (1988).
6. Smith, C. and Carpenter, P.W. The effect of solid surfaces on turbulent jet noise, J. Sound and Vibration, 185(3), 397-413, (1995).
7. Carpenter, P.W. and Smith, C. The aeroacoustics and aerodynamics of high-speed Coanda devices, Part 2: Effects of modifications for flow control and noise reduction, J. Sound and Vibration, 208(5), 803-822., (1997).
8. Green, P.N., The Fluid Dynamics and Aeroacoustics of External Coanda Flares, PhD Thesis, Exeter, (1987).
9. Harper-Bourne, M and Fisher, M.J., The Noise from Shock Waves in Supersonic Jets, Proc. AGARD Conf. on Noise Mechanisms, CP-131, Paper 11, (1973).